Reducing-end “clickable” functionalizations of chitosan oligomers for the synthesis of chitosan-based diblock copolymers

Amani Moussa, Agnès Crépet, Catherine Ladavière, Stéphane Trombotto

Article

Reducing-end "clickable" functionalizations of chitosan oligomers for the synthesis of chitosan-based diblock copolymers

Amani Moussa, Agnès Crépet, Catherine Ladavière, Stéphane Trombotto*

Ingénierie des Matériaux Polymères (IMP, UMR 5223 - CNRS), Université Claude Bernard Lyon 1, Univ Lyon, F-69622 Villeurbanne, France

* Corresponding author at: Ingénierie des Matériaux Polymères (IMP@Lyon1, UMR 5223), campus LyonTech-La Doua, bâtiment Polytech, 15 bd A. Latarjet, 69622 Villeurbanne cedex, France.
E-mail address: stephane.trombotto@univ-lyon1.fr (S. Trombotto)

Abstract: Chitooligosaccharides (COS) produced by nitrous acid depolymerization of chitosan are unique chitosan oligomers due to the presence of the 2,5-anhydro-D-mannofuranose (amf) unit at their reducing end. In this work, we focused on the reductive amination and the oximation of the amf aldehyde group towards various functionalized anilines, hydrazides and *O*-hydroxylamines. The aim of this work was to synthesize new COS-based building blocks functionalized at their reducing end by different "clickable" chemical groups such as alkene, alkyne, azide, hydrazide and thiol. Targeted functionalized COS were synthesized in excellent mass yields and fully characterized by NMR spectroscopy and MALDI-TOF mass spectrometry. Our results showed these functionalizations are quantitative, versatile and can be easily performed in mild reaction conditions. Finally, these COS-based building blocks could be useful intermediates for the development of advanced functional COS-based conjugates, as illustrated in this work by the synthesis of new COS-poly(ethylene glycol) (PEG) diblock copolymers.

Keywords: nitrous deamination; reducing-end functionalization; chitosan oligomer-based building block; click chemistry; diblock copolymer;

1. Introduction

Chitosan is a linear polysaccharide, copolymer of (1→4)-linked units of 2-amino-2-deoxy-β-D-glucopyranose (GlcN) and 2-acetamido-2-deoxy-β-D-glucopyranose (GlcNAc) (Yeul, & Rayalu, 2013). Although naturally present in *Mucoraceae* fungi, chitosan is obtained industrially by thermochemical *N*-deacetylation of chitin, a structural polysaccharide widely present in arthropod exoskeletons and cephalopod endoskeletons (Younes, & Rinaudo, 2015). Over the past decades, chitosan has received more attention as a functional biopolymer due to its biocompatibility, biodegradability and numerous biological activities (Hamed, Ozogul, & Regenstein, 2016). Chitosan and their derivatives have been proposed for applications including agriculture, biomedicals, cosmetics and food (Dash, Chiellini, Ottenbrite, & Chiellini, 2011; Hamed *et al.*, 2016). However many applications of chitosan are often hampered by its high viscosity in dilute aqueous acid solutions or its poor solubility in neutral and basic pH solutions. Consequently, a growing interest has been shown to chitooligosaccharides (COS) defined as oligomer forms of chitosan or chitin. In comparison with chitosan, COS show a better water solubility and a lower viscosity in aqueous solutions, in addition to several specific biological properties, such as antibacterial, antifungal and antitumour activities, as well as immuno-enhancing effects on animals (Li, Xing, Liu, & Li, 2016; Liaqata, & Eltemb, 2018; Mourya, Inamdar, & Choudhari, 2011; Xia, Liu, Zhang, & Chen, 2011). COS have also been shown to elicit increasing protective responses in various plants and possess antimicrobial activities against a wide spectrum of phytopathogens (Das *et al.*, 2015). Conventional methods for preparing COS are either chemical or enzymatic. Chemical methods consist of the depolymerization of chitin or chitosan including mainly hydrochloric acid hydrolysis, nitrous acid deamination, fluorolysis in anhydrous hydrogen fluoride, and oxidative-reductive reaction by hydrogen peroxide for instance (Mourya *et al.*, 2011). Additionally, total chemical syntheses of COS, involving multiple protection and deprotection steps, have also been reported (Yang, & Yu, 2014). Enzymatic methods include the hydrolysis of chitin and chitosan with hydrolytic enzymes and the synthesis of COS by means of enzymes having transglycosylation activities (Aam *et al.*, 2010).

Besides, chemical functionalizations of COS are currently being explored intensively in order to design new properties and to develop advanced functional COS-based conjugates (Liaqata *et al.*, 2018; Lodhi *et al.*, 2014). In particular, the functionalization of COS with "clickable" chemical groups is of primary interest, based on the robustness, high efficiency, compatibility with sensitive functional groups and versatility of "click" reactions, such as Cu(I)-mediated azide/alkyne cycloadditions (CuAAC) (Guerry *et al.*, 2013; Huang *et al.*, 2009; Marzaioli *et al.*, 2012) or thiol/ene additions (Illy *et al.*, 2014). A convenient route for the incorporation of

"clickable" groups into COS is based on the reactivity of amine groups along the oligosaccharide backbone (Huang *et al.*, 2009; Illy *et al.*, 2014; Marzaioli *et al.*, 2012). However, as inherent physico-chemical and biological properties of COS are closely related to the presence of free amine groups, this simple strategy is often unfavorable for many applications. In order to circumvent the use of amine groups and to preserve the chemical nature of COS backbones, an alternative approach consists of exploiting the presence of the aldehyde group at the reducing end of COS. Thus, Guerry *et al.* (2013) have shown that alkyne-bearing aniline constituted a powerful tool for the easy derivatization of COS and the preparation of novel chitosan oligosaccharide-based advanced materials.

Surprisingly, this reducing-end approach has rarely been investigated for the introduction of "clickable" chemical groups in COS produced by nitrous acid depolymerization of chitosan (Pickenhahn, Grange, De Crescenzo, Lavertu, & Buschmann, 2017). These COS are indeed particularly advantageous since their reducing-end unit is composed of a 2,5-anhydro-D-mannofuranose (amf) moiety (Liu, Tokura, Nishi, akairi, 2003; Strand, Issa, Christensen, Vårum, & Artursson, 2008; Tømmeraas, Vårum, Christensen, & Smidsrød, 2001; Pickenhahn *et al.*, 2015). In comparison with GlcNAc and GlcN, amf does not mutarotate in aqueous solution and the aldehyde group is more available for reactions since it does not participate in intramolecular hemiacetals. Furthermore, the nitrous acid depolymerization can be performed in aqueous medium under mild conditions and the extent of depolymerization can be controlled through the stoichiometry of reaction. Finally, thanks to this depolymerization method, chitosan oligomers can be easily prepared in gram scale quantity (Hussain, Singh, & Chittenden, 2012; Mourya, Inamdar, & Choudhari, 2011).

As part of our investigations about the preparation of functionalized chitosan oligomer derivatives (Abla *et al.*,2013; Moussa, & Trombotto, 2016; Salim, Ailincai, & Trombotto, 2014; Salim, Galais, & Trombotto, 2014), herein we report the synthesis of new COS-based building blocks functionalized at their reducing ends with various "clickable" chemical groups, such as alkene, alkyne, azide, hydrazide and thiol. Reducing-end derivatizations were performed by reaction of the COSamf aldehyde group with the amine group of anilines, hydrazides and O-hydroxylamines bearing different "clickable" groups. The aim of the present study is to demonstrate that numerous "clickable" COS-based building blocks can be easily obtained from COS produced by nitrous acid depolymerization of chitosan and can be used for the preparation of high potential COS-based conjugates, as illustrated in this work by the synthesis of new COS-*b*-PEG copolymers.

2. Materials and methods

2.1. Materials

Commercial chitosan (batch 244/020208; degree of *N*-acetylation (DA) ~ 0%; M_w = 270,000 g/mol; M_n = 115,000 g/mol; Đ = 2.3) was supplied by Mahtani Chitosan Ltd (Veraval, India). Methoxypolyethylene glycol succinimidyl carboxymethyl ester (mPEG-NHS ester, M_n = 2,000 g/mol, Đ = 1.01, purity > 95%) was provided by Jenkem Technology (Plano, USA). Sodium nitrite (purity > 99%), 4-(propargyloxy)aniline (purity > 95%), 4-(mercapto)aniline (purity > 97%), 4-(azido)aniline (purity > 97%), *O*-Allylhydroxylamine hydrochloride (purity > 98%), *O*-2-Propynylhydroxylamine hydrochloride (purity > 98%), adipic dihydrazide (purity > 98%), succinic dihydrazide (purity > 96%), sodium cyanoborohydride (purity > 95%), deuterium oxide (D_2O, purity > 99.96% atom D), methoxypolyethylene glycol azide (mPEG-azide, M_n = 2,000 g/mol, Đ = 1.02, purity > 95%) and all others chemicals and solvents were provided by Sigma-Aldrich (Saint-Quentin Fallavier, France).

2.2. Characterization methods

2.2.1 NMR spectroscopy

^1H and ^{13}C NMR spectra were recorded on a Bruker 500 MHz spectrometer at 300 K. All samples were dissolved at 10 mg/mL in D_2O with 5 µL HCl 12 N, and transferred to 5 mm NMR tubes. Trimethylsilyl-3-propionic-2,2,3,3-D_4 acid sodium salt (99% atom D, TMSPA from Sigma-Aldrich, Saint-Quentin Fallavier, France) was used as internal reference (δ 0.00 and -2.25 ppm for ^1H and ^{13}C NMR, respectively). ^1H NMR spectral data are presented as follows: chemical shifts (δ ppm downfield from TMSPA), multiplicity (s = singlet, d = doublet, t = triplet, m = multiplet), coupling constants (Hz), integration, proton assignment. ^{13}C NMR spectral data are presented as follows: chemical shifts (δ ppm), carbon assignment. Proton and carbon signals were assigned thanks to 2D NMR techniques (*i.e.* COSY, HSQC and HMBC).

2.2.2. MALDI-TOF mass spectrometry

MALDI-TOF mass spectra were acquired with a Voyager-DE STR (AB Sciex, Framingham, MA) equipped with a nitrogen laser emitting at 337 nm with a 3 ns pulse. The instrument was operated in the linear or reflectron mode. Ions were accelerated to a final potential of 20 kV. The positive ions were detected in all cases. Mass spectra were the sum of 300 shots and an external mass calibration of mass analyzer was used (mixture of peptides from Sequazyme™ standards kit, AB Sciex). The matrix used for all experiments was 2,5-dihydroxybenzoic acid (DHB) purchased from Sigma-Aldrich and used directly without further purification. The

solid matrix and samples were dissolved at 10 mg/mL in water. A volume of 45 µL matrix solution was then mixed with 5 µL of sample solutions. An aliquot of 0.5 µL of each resulting solution was spotted onto the MALDI sample plate and air-dried at room temperature.

2.2.3. Size-exclusion chromatography (SEC)

SEC was performed on a chromatographic equipment composed of a 1260 Infinity Agilent Technologies pump connected to two TSK gel G2500 and G6000 columns (Tosoh Bioscience) in series. A multi-angle light scattering (MALS) detector HELEOS II (Wyatt Technology) operating at 664 nm was coupled on line to a Wyatt Optilab T-Rex differential refractometer. Sample solutions at 2-5 mg/mL were prepared and eluted in AcOH (0.2 M)/$AcONH_4$ (0.15 M) buffer (pH 4.5). Solutions were previously filtered through 0.45 µm pore size membranes (Millipore) before injection. The eluent flow rate was 0.5 mL/min. The values of the refractive index increment dn/dc used for molar mass calculations were equal to: (*i*) 0.198 mL/g for commercial chitosan and COSamf samples, (*ii*) 0.169 and 0.164 mL/g for the copolymers **18** and **19**, respectively.

3. Results and discussion

3.1. Preparation of COSamf by nitrous acid depolymerization of chitosan

The nitrous acid depolymerization is a well-known chemical method for the preparation of low molar mass chitosans (Allan, & Peyron, 1989). This reaction can be performed in aqueous solution under mild conditions of temperature and acidity and is specific to GlcN units. Thus, this is a homogeneous reaction where the number of glycosidic bonds broken is roughly stoichiometric to the amount of nitrous acid used (Hussain *et al.*, 2012). Briefly, the depolymerization mechanism involves the reaction of nitrous acid with the amine group of the GlcN unit, leading to *(i)* the release of N_2, *(ii)* the breaking of the GlcN unit glycosidic linkage and *(iii)* the transformation of the GlcN unit into 2,5-anhydro-D-mannofuranose at the new reducing end (Scheme 1).

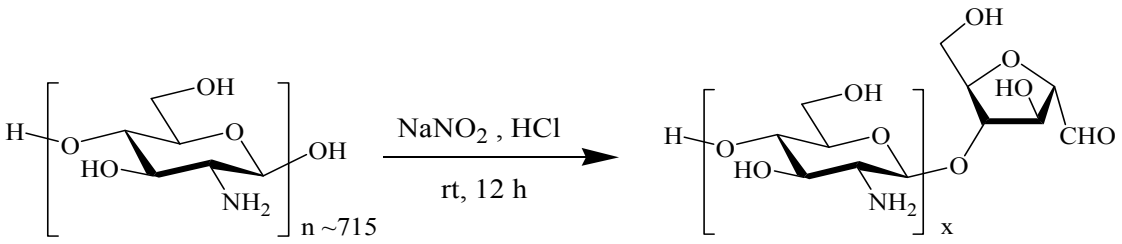

Chitosan (DA ~ 0%)

COSamf: **1** (x ~10)
2 (x ~22)
3 (x ~45)

Scheme 1. Synthesis of COSamf **1-3** by nitrous acid depolymerization of fully *N*-deacetylated chitosan

In this study, the nitrous acid depolymerization of fully *N*-deacetylated chitosan was used to produce three COSamf samples **1-3** with an average number of GlcN repeating units (x) ranging from 10 to 45 (Scheme 1). The nitrous acid depolymerization was typically performed by mixing a dilute aqueous acid solution of chitosan and a specific molar quantity of $NaNO_2$ at room temperature for 12 h, as described in our previous studies (Salim *et al.*, 2014; Salim *et al.*, 2014; Moussa *et al.*, 2016). At the end of the reaction, COSamf samples were isolated and purified by precipitation using appropriate conditions according to x values. Thus, COSamf **2** (x ~22) and **3** (x ~45) were easily precipitated by increasing the pH of the solution by addition of ammonia until pH ~8-9. Since COSamf **1** (x ~10) showed good water solubility whatever the pH, it was advantageously precipitated in acetone. Finally, COSamf **1-3** were produced in gram-scale quantities with mass yields ranging from 80 to 85% after purification (Table 1).

Table 1. Characterization data of synthesized COSamf **1-3**

Sample	GlcN unit/$NaNO_2$ molar ratio	Mass yield (%)	x [a]	M_w [b] (g/mol)	M_n [b] (g/mol)	Đ [b]
COSamf **1**	4	80	10 ±1	2.33×10^3	2.08×10^3	1.12
COSamf **2**	10	82	22 ±2	3.89×10^3	3.38×10^3	1.15
COSamf **3**	30	85	45 ±2	9.98×10^3	7.74×10^3	1.29

(a) The average number of GlcN repeating unit (x) in COSamf was determined by ^{1}H NMR in D_2O at 300 K; (b) weight- and number-average molar masses (M_w and M_n, respectively) and dispersity value (Đ) were determined by SEC-MALS. Molar masses results were expressed as means of ± 10%.

The expected chemical structure of COSamf **1-3** was fully confirmed by ^{1}H and ^{13}C NMR spectroscopy and MALDI-TOF mass spectrometry (MS) analyses. Thanks to two-dimensional NMR analyses, all ^{1}H and ^{13}C resonances corresponding to GlcN and amf units of COSamf were assigned (Figure S5 in Supplementary data). As shown in Figure 1a, the ^{1}H NMR spectrum of COSamf **2** presents high intensity signals assigned to GlcN protons at 4.87 ppm for H-1 (GlcN), between 4.07 and 3.62 ppm for H-3 to H-6 (GlcN) and at 3.15 ppm for H-2 (GlcN). The presence of the amf unit at the reducing end is confirmed by four typical low intensity signals at 5.10, 4.45, 4.23 and 4.13 ppm assigned to H-1 (amf), H-3 (amf), H-4 (amf) and H-5 (amf), respectively. These assignments corroborate previous NMR data published for analogous COSamf structures (Tømmeraas *et al.*, 2001; Pickenhahn *et al.*, 2015). Moreover, the ^{1}H NMR spectrum shows clearly two other low intensity signals assigned to H-4 and H-5 of the GlcN unit neighboring of the amf unit at 3.50 and 3.55 ppm, respectively. In addition, the ^{13}C NMR spectrum of COSamf **2** presents high intensity peaks assigned to GlcN units and low intensity peaks corresponding to both the reducing-end amf unit and the GlcN unit linked to the amf unit (Figure 1b). It is worth mentioning that neither the ^{1}H spectrum nor the ^{13}C spectrum showed the resonances expected for the free aldehyde group of the amf residue (*i.e.* ^{1}H: ca. 9.49 ppm and ^{13}C: ca. ~180 ppm) (Tømmeraas *et al.*, 2001). Thus, the H-1 (amf) and C-1 (amf) resonances at 5.10 and 89.5 ppm, respectively, pointed out that the aldehyde moiety appears to be present only in its hydrated form $-CH(OH)_2$ in the NMR conditions used in this study (RT, pH < 3), as already observed by Pickenhahn *et al.* (2015). Finally, COSamf **1, 2** and **3** led to similar ^{1}H and ^{13}C spectra with comparable assignments.

For each COSamf, the average GlcN repeating unit number (x) given in Table 1 was determined by ^{1}H NMR spectroscopy from the relative peak intensities of H-3 (amf) and H-2 (GlcN) signals at 4.45 and 3.15 ppm (Figure 1a), respectively, according to the formula (1):

$$x = \frac{I_{H-2\ (GlcN)}}{I_{H-3\ (amf)}} \qquad (1)$$

Additionally, COSamf **1-3** were also characterized by SEC-MALS according to their weight- and number-average molar masses (M_w and M_n, respectively) and dispersity values (Đ) in Table 1. The average GlcN repeating unit number (x) estimated by the ^{1}H NMR spectroscopy and SEC-MALS measurements linearly increased by increasing the GlcN unit/$NaNO_2$ molar ratio in the nitrous acid depolymerization reactions (Fig. 2).

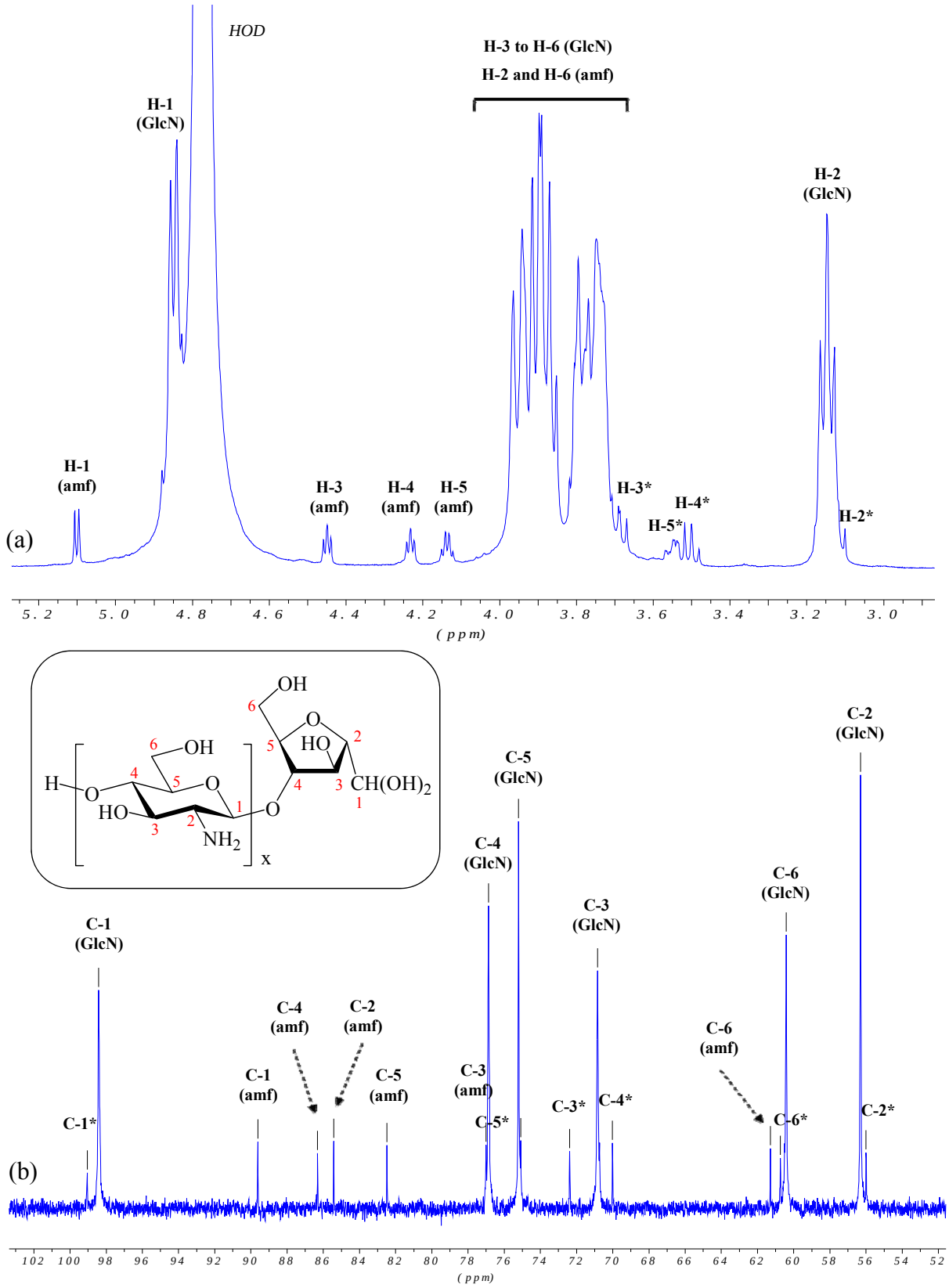

Figure 1. (a) ^{1}H NMR spectrum (500 MHz) and (b) ^{13}C NMR spectrum (125 MHz) of COSamf **2** (x ~22) in D_2O at 300 K. H and C atoms of the GlcN unit linked to the amf unit are indicated by an asterisk.

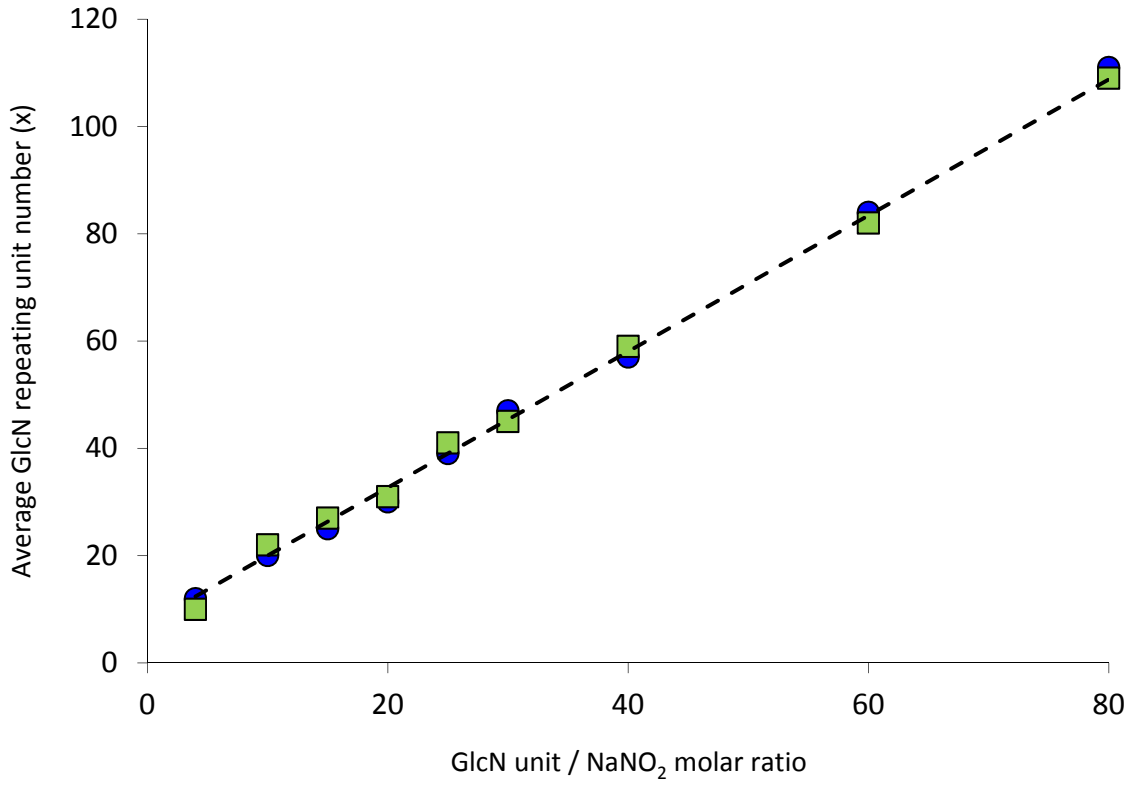

Figure 2. Relationship between the GlcN unit/$NaNO_2$ molar ratio and the average GlcN repeating unit number (x) of COSamf. Fully *N*-deacetylated chitosan (2 % w/w) was depolymerized by sodium nitrite in 0.15M hydrochloric acid solution for 12 h at room temperature. x values were estimated by: (■) ^{1}H NMR from relative peak intensities of H-3 (amf) and H-2 (GlcN) signals at 4.45 and 3.15 ppm, respectively (see Figure 1) according to the formula $x = (I_{H\text{-}2(GlcN)} / (I_{H\text{-}3(amf)})$; (●) SEC-MALS from the measured number-average molar mass (M_n) of COSamf and the molar mass of the GlcN repeating unit (M_0 = 161 g/mol) according to the formula $x = (M_n\text{-}162) / M_0$. Results are expressed as means ± 5%.

3.2. Functionalizations of COSamf reducing ends

The aim of this study is to show the potential reactivity of the aldehyde group of COSamf towards several functionalized amine derivatives, so as to generate original COS-based building blocks with "clickable" groups at their reducing ends. Amine derivatives were selected from aniline, *O*-hydroxylamine and hydrazide derivatives due to their lower pKa values (*ca* 3-6) in comparison with chitosan oligomers (pKa ~6.5-7). Hence, we expected that amine groups of these derivatives are more nucleophilic than amine groups of COSamf towards aldehyde groups in slightly acid conditions (pH ~5.5) required for the complete solubilization of COSamf in aqueous solutions. Thus, chemical functionalizations of COSamf reducing ends were carried out by means of reductive amination and oximation using above-

mentioned amine derivatives bearing different "clickable" chemical groups, such as alkene, alkyne, azide, hydrazide and thiol, as illustrated in Scheme 2.

3.2.1. Reductive amination of COSamf with functionalized anilines

The reactivity of COSamf towards aniline derivatives has been studied through the reductive amination of COSamf with three different functionalized anilines, *i.e.* 4-(propargyloxy)aniline, 4-(mercapto)aniline and 4-(azido)aniline (pathways a, b, c in Scheme 2, respectively). Thus, the reductive amination of COSamf **2** (x ~22) by an excess of 4-(propargyloxy)aniline (2 eq./amf unit) was carried out in the presence of $NaBH_3CN$ in ammonium acetate buffer (0.15 M, pH 5.5) at 40°C for 2 days, based on reaction conditions described by Guerry *et al.* (2013) (pathway a in Scheme 2). The functionalized COSamf **5** was isolated in 90% mass yield by precipitation in basic conditions by addition of concentrated ammonia. The NMR spectroscopy and MALDI-TOF MS analyses were in complete agreement with the expected chemical structure of the compound **5**, indicating that the functionalization reaction is quantitative. Indeed, thanks to 2D NMR analyses, all resonances of ^{1}H and ^{13}C NMR spectra were assigned (Figure S16 in Supplementary data). Thus, the ^{1}H NMR spectrum showed clearly the occurrence of CH_2N protons at 3.40-3.25 ppm, in addition to the presence of the alkyne proton (C≡CH) at 2.95 ppm. Additionally, the ^{13}C NMR spectrum of the compound **5** showed a signal at 46.9 ppm corresponding to the CH_2N carbon and two signals at 79.5 and 77.2 ppm for C≡CH carbons. Thus, both ^{1}H and ^{13}C NMR analyses confirmed the coupling reaction between the COSamf aldehyde group and the amine group of the aniline derivative. Besides, the ^{1}H NMR analysis allowed us to determine the x value of COSamf **5** (*i.e.* x ~23) taking into account signal intensities of both H-2 (GlcN) and aromatic protons. This result confirmed that the reductive amination condition used in this study did not hydrolyze the oligomer chain of the starting COSamf **2** (x ~22). In similar reaction conditions, the reductive amination of COSamf **1** (x ~10) and **3** (x ~45) with 4-(propargyloxy)aniline led also to expected functionalized COSamf **4** (x ~12) and **6** (x ~46) in 87 and 89% mass yields, respectively. However, when applying these reaction conditions with propargylamine as starting amine, the expected functionalized COSamf was not obtained. This result can be explained by the protonation of the amine group of propargylamine (pKa ~10.6) in the reaction conditions (pH ~5.5), which makes the amine group not reactive enough towards the COSamf aldehyde.

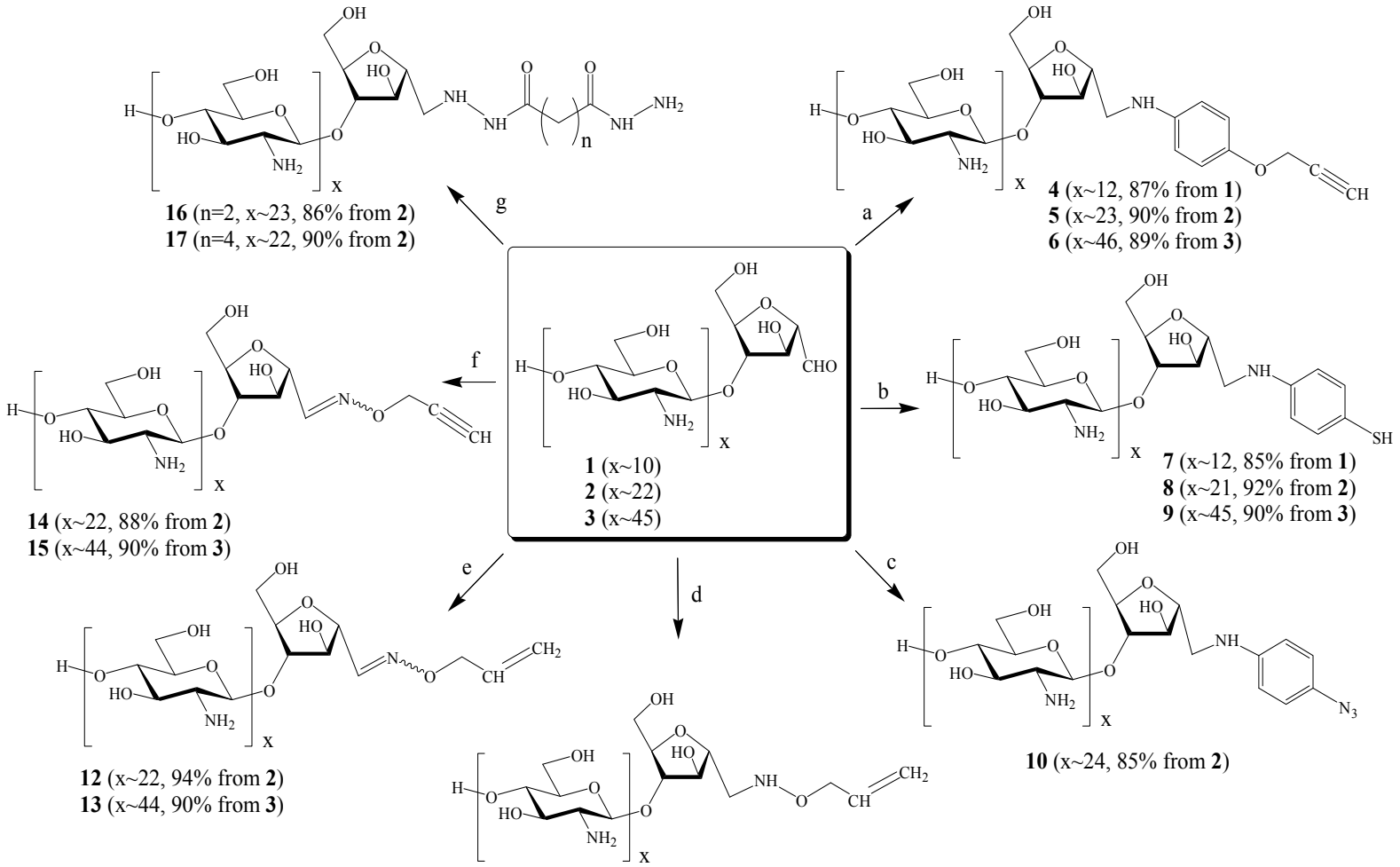

Scheme 2. Pathways of the reducing-end functionalization of COSamf with various functionalized amine derivatives: (a) 4-(propargyloxy)aniline, $NaBH_3CN$, ammonium acetate buffer (pH 5.5)/ethanol, 2 days, 40°C; (b) 4-(mercapto)aniline, $NaBH_3CN$, ammonium acetate buffer (pH 5.5)/ethanol, 2 days, 40°C; (c) 4-(azido)aniline, $NaBH_3CN$, ammonium acetate buffer (pH 5.5), 2 days, 40°C; (d) *O*-allylhydroxylamine, $NaBH_3CN$, acetic acid (pH 4.5)/DMSO, 3 days, 40°C; (e) *O*-allylhydroxylamine, acetic acid (pH 4.5)/DMSO, 2 days, 40°C; (f) *O*-propynylhydroxylamine, acetic acid (pH 4.5)/DMSO, 2 days, 40°C; (g) succinic dihydrazide, $NaBH_3CN$, ammonium acetate buffer (pH 5.5), 2 days, RT; adipic dihydrazide, $NaBH_3CN$, ammonium acetate buffer (pH 5.5), 2 days, 40°C. Note that % values given in brackets correspond to mass yields.

In the same way, the reductive amination of COSamf **1-3** with 4-(mercapto)aniline led to expected 4-(mercapto)aniline-linked COSamf **7-9** in 85-92% mass yields (Scheme 2). Moreover, the reducing end of COSamf **2** (x ~22) could also be functionalized by an azido group in 85% mass yield using 4-(azido)aniline (Scheme 2, compound **10** (x ~24)).

3.2.2. Reductive amination and oximation of COSamf with O-functionalized hydroxlyamines

The reactivity of COSamf towards *O*-functionalized hydroxylamine derivatives has been investigated through the coupling reactions of COSamf with *O*-allylhydroxylamine (pathways d and e in Scheme 2) and *O*-propynylhydroxylamine (pathway f in Scheme 2) by reductive amination or oximation.

a) Reductive amination with O-allylhydroxylamine. The reductive amination of COSamf **2** (x ~22) was carried out with an excess of *O*-allylhydroxylamine (10 eq./amf unit) in the presence of $NaBH_3CN$ in a mixture of aqueous acetic acid (1.5% w/v, pH 4.5)/DMSO (3:1 v/v) at 40°C for 2 days. *O*-allylhydroxylamine-linked COSamf **11** (x ~22) was isolated in 85% mass yield by precipitation in basic conditions (pH ~8-9) by addition of concentrated ammonia (Scheme 2). Thanks to 2D NMR analyses, all ^{1}H and ^{13}C resonances of the compound **11** were assigned confirming the reductive amination of the amf aldehyde group with *O*-allylhydroxylamine (Figure S34 in Supplementary data). The ^{1}H NMR spectrum showed clearly the occurrence of CH_2N protons at 3.10 ppm in addition to the presence of alkene protons ($CH=CH_2$) at 5.95 and 5.40-5.25 ppm. Moreover, the ^{13}C NMR spectrum of the compound **11** showed a signal at 52.7 ppm corresponding to the CH_2N carbon and two signals at 133.9 and 119.7 ppm for CH= and $=CH_2$ carbons, respectively. Furthermore, MALDI-TOF MS analyses confirmed the chemical structure of the compound **11** (Figure S35 in Supplementary data).

b) Oximation with O-allylhydroxylamine. The possibility to link directly COSamf **2** with *O*-allylhydroxylamine without the need of the $NaBH_3CN$ reduction step was also studied. Typically, the oximation of COSamf **2** (x ~22) was carried out in aqueous acetic acid (1.5% w/v, pH 4.5) with an excess of *O*-propynylhydroxylamine (10 eq./amf unit) solubilized in DMSO at 40°C for 2 days, leading to the compound **12** (x ~22) in 96% mass yield (Scheme 2). The expected chemical structure of the compound **12** was fully determined by ^{1}H and ^{13}C NMR analyses and confirmed by MALDI-TOF MS analyses (Figure S39 in Supplementary data). In comparison with the compound **11**, the ^{1}H and ^{13}C NMR spectra showed the presence of the imine group ($CH_2=N$, in *E* and *Z* isomers) at 7.65/7.05 ppm and 152.4/150.6 ppm, respectively. As for the reductive amination, it seems that the oximation reaction did not affect the COS backbone, since the x value of compound **12** and COSamf **2** (x ~22) did not

change. Additionally, successful coupling was also observed for the oximation between *O*-allylhydroxylamine and COSamf with higher x values (COSamf **3**, x ~45) leading to the targeted compound **13** (x ~44) in 95% mass yield (Scheme 2).

c) Oximation with O-propynylhydroxylamine. The grafting of an alkyne group into the reducing-end unit of COSamf was also studied by using *O*-propynylhydroxylamine according to similar oximation conditions described for the compound **12**. In these conditions, the targeted compound **14** (x ~22) was obtained in 88% mass yield from COSamf **2** (x ~22) (Scheme 2). The NMR and MALDI-TOF MS analyses of the compound **14** were found to be in complete agreement with the expected chemical structure (Figures S41 to S44 in Supplementary data). The ^{1}H NMR spectrum of the compound **14** showed the occurrence of CH_2=N protons as a mixture of *E* and *Z* isomers at 7.65 and 7.10 ppm, in addition to the presence of the alkyne proton (C≡CH) at 2.90 ppm. Moreover, the ^{13}C NMR spectrum showed two signals at 153.8 and 151.8 ppm corresponding to the CH_2=N carbon (*E* and *Z* isomers) and two signals at 79.9 and 76.7 ppm for both C≡CH carbons. In the same manner, the oximation between *O*-propynylhydroxylamine and COSamf with higher x values (COSamf **3**, x ~45) was successfully performed, leading to the targeted compound **15** (x ~44) in 90 % mass yield (Scheme 2).

3.2.3. Reductive amination of COSamf with hydrazides

The reactivity of COSamf towards hydrazide derivatives has been investigated through the reductive amination of COSamf **2** by two commercial hydrazides, *i.e.* succinic and adipic dihydrazides (pathway g, Scheme 2). Thus, the reductive amination of COSamf **2** by succinic dihydrazide was carried out with a large excess of dihydrazide in order to promote the coupling reaction with one hydrazide group only. Typically, COSamf **2** (x ~22) and succinic dihydrazide (10 eq./amf unit) were fully solubilized in ammonium acetate buffer (pH 5.5). The mixture was stirred at room temperature for 1 day, and then $NaBH_3CN$ was added in excess to the solution. After stirring during 1 day at room temperature, the addition of concentrated ammonia (28% w/w) resulted in the precipitation of the expected compound **16** (x ~23) in 86% mass yield (Scheme 2). The chemical structure of the compound **16** was confirmed by NMR spectroscopy and MALDI-TOF MS analyses. Thus, ^{1}H and ^{13}C NMR spectra were fully characterized thanks to 2D NMR analyses, showing the coupling reaction between the COSamf aldehyde group and the hydrazide amine (Figures S46 to S48 in Supplementary data). Thus, NMR analyses showed signals at 3.05 and 52.4 ppm in ^{1}H and ^{13}C NMR spectra, respectively assigned to the presence of the CH_2N group. This result is in good agreement with a single coupling between COSamf and succinic dihydrazide, as

confirmed also by MALDI-TOF MS analyses (Figure S49 in Supplementary data). In the same way, the reductive amination of COSamf **2** was studied with adipic dihydrazide. In this case, best coupling conditions were obtained at 40°C in comparison with room temperature for succinic dihydrazide, leading to the expected compound **17** (x ~22) in 90% mass yield (Scheme 2).

3.3. Preparation of COS-b-PEG copolymers

To illustrate the potential of these COS-based building blocks for the development of functional COS-based conjugates, we further investigated the synthesis of COS-PEG diblock copolymers. Despite the huge interest of PEGylated chitosan assemblies as cationic nanocarriers for the delivery of drugs, genes and siRNA, the synthesis of chitosan-PEG diblock copolymers has rarely been studied in the literature compared with chitosan-PEG graft copolymers (Casettari et al., 2012). However, as mentioned by Novoa-Carballal and Müller (2012), block copolymers present several advantages in comparison with graft copolymers, such as: (*i*) they preserve the chemical structure of the polysaccharide (none of its lateral groups are modified), and therefore its biological properties, and (*ii*) they seem to enable a much greater control of the nanostructure assembly than graft copolymers do. Concerning the synthesis of chitosan-PEG block copolymers, only few chemical methods were currently reported in the literature. Thus, Ganji and Abdekhodaie (2008) described the first preparation of chitosan-PEG diblock copolymers by introducing an acrylate PEG macromer onto the chitosan chain by means of a radical depolymerization process using potassium persulfate as initiator. Then, Novoa-Carballal and Müller (2012) proposed the synthesis of chitosan-PEG diblock copolymers by oxime condensation of aminooxy PEG and the reducing end of chitosan. More recently, Pickenhahn *et al.* (2017) developed a novel regioselective thioacetylation of chitosan end-groups for the synthesis of chitosan-*b*-PEG_2 block copolymers.

In this study, COS-PEG diblock copolymers **18** and **19** were synthesized according to two different end-to-end click reactions (Scheme 3). The first way was based on the CuAAC click reaction using the terminal alkyne-functionalized COS building block **5** and a commercial mPEG-azide (M_n = 2,000 g/mol). The coupling reaction was performed under similar CuAAC conditions ($CuSO_4$/sodium ascorbate) described by Guerry *et al.* (2013) leading to the diblock copolymer **18** (M_n = 6,520 g/mol, Đ = 1.26, see Table 2) with an overall mass yield of 72% after purification. However, it worth noting that the use of copper catalyst in the synthesis of COS-PEG diblocks could be a drawback, considering that (*i*) chitosan can present a strong affinity with copper ions (Rhazi *et al.*, 2001) and (*ii*) the copper contamination in COS-based

conjugates can limit their biomedical applications (Kalia and Raines, 2010). Consequently, in order to overcome this limitation, we have investigated an alternative strategy for the synthesis of COS-PEG diblock copolymers free of copper ions. Thus, the synthesis of COS-*b*-PEG **19** (M_n = 6,330 g/mol, Đ = 1.15, see Table 2) was carried out by hydrazide condensation of the COS building block **17** with a commercial mPEG-NHS ester (M_n = 2,000 g/mol) in 70% mass yield after purification (Scheme 3). In both syntheses, COS-*b*-PEG copolymers were advantageously isolated after several washings in ethanol and dialyses to remove the excess of PEG starting material. The absence of free PEG in diblock copolymer samples was observed by SEC (Figures S55 and S57 in Supplementary data). Chemical structures of copolymers were confirmed by ^{1}H NMR spectroscopy which indicated the expected resonances that are distinctive for each block (Figures S54 and S56 in Supplementary data). In particular, for the diblock copolymers **18**, a characteristic peak of the triazole ring proton around 8.2 ppm demonstrated the coupling reaction (Guerry *et al.*, 2013).

Table 2. Characterization data of COS-*b*-PEG copolymers **18** and **19** and their corresponding COS-based building blocks **5** and **17** (see Scheme 3).

Sample	M_w **(g/mol)** [a]	M_n **(g/mol)** [a]	**Đ** [a]
Building block **5**	4.86×10^3	4.23×10^3	1.15
COS-*b*-mPEG **18**	8.21×10^3	6.52×10^3	1.26
Building block **17**	4.41×10^3	3.94×10^3	1.12
COS-*b*-mPEG **19**	7.28×10^3	6.33×10^3	1.15

(a) weight- and number-average molar masses (M_w and M_n, respectively) and dispersity value (Đ) were determined by SEC-MALS. Molar masses results were expressed as means of ± 10%.

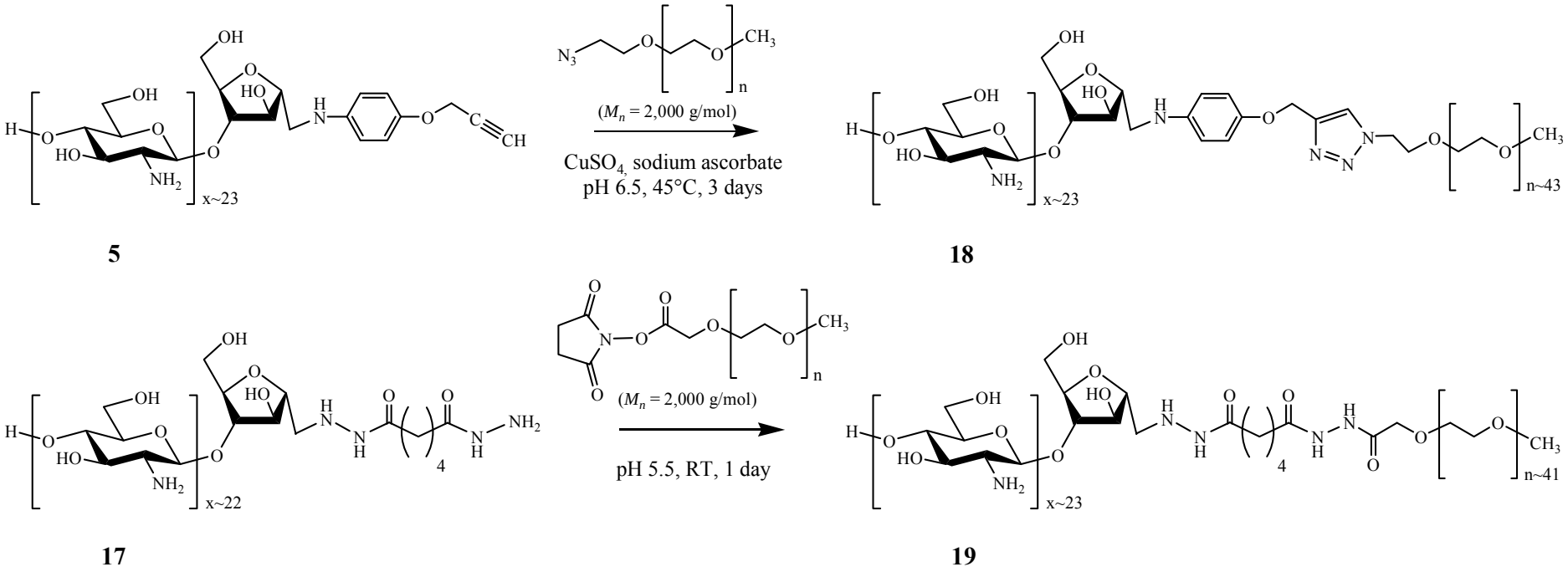

5 **18**

17 **19**

Scheme 3. Chemical syntheses of COS-*b*-PEG copolymers **18** and **19**

4. Conclusion

COSamf compounds with a well-defined average number of GlcN repeating units (x) ranging from 10 to 45 were easily synthesized by nitrous acid depolymerization of fully *N*-deacetylated chitosan. Then, the reducing-end functionalization of these COSamf was performed based on the reactivity of the aldehyde group of the amf unit. Thus, reductive amination and oximation with various "clickable" functionalized aniline, *O*-hydroxylamine and hydrazide derivatives led to expected COS-based building blocks in excellent mass yields. Building blocks were fully characterized by NMR spectroscopy and MALDI-TOF mass spectrometry. In this study, we showed that our strategy for the chemical reducing-end functionalization of chitosan oligomers is powerful and versatile. Thus, the introduction of various "clickable" chemical groups (*e.g.* alkene, alkyne, azide, hydrazide and thiol) can be quantitatively carried out from COSamf in one reaction step only. These promising results open the way for the preparation of high potential COS-based conjugates, as illustrated in this work by the synthesis of new COS-*b*-PEG diblock copolymers.

Acknowledgments

This work has benefited from the facilities and expertise of the Liquid Chromatography for Polymers and NMR platforms of the Institut de Chimie de Lyon for the structural characterization of synthesized compounds.

Appendix A. Supplementary data

Supplementary data (synthesis methods and structural characterizations by NMR spectroscopy, MALDI-TOF mass spectrometry and size-exclusion chromatography) associated with this article can be found, in the online version, at http://…

References

Aam, B.B., Heggset, E.B., Norberg, A.L., Sørlie, M., Vårum, K.M., & Eijsink, V.G.H. (2010). Production of chitooligosaccharides and their potential applications in medicine. *Marine Drugs*, *8*, 1482-1517.

Abla, M., Marmuse, L., Delolme, F., Vors, J.-P., Ladavière, C., & Trombotto, S. (2013). Access to tetra-N-acetyl-chitopentaose by chemical N-acetylation of glucosamine pentamer. *Carbohydrate Polymers*, *98*, 770-777.

Allan, G. G., & Peyron, M. (1989). The kinetics of the depolymerization of chitosan by nitrous acid. In G. Skjak-Bræk, T. Anthonsen, & P. Sandford (Eds), *Chitin and chitosan: sources, chemistry, biochemistry, physical-properties and applications* (pp. 443–466). Springer Netherlands.

Casettari, L., Vllasaliu, D., Castagnino, E., Stolnik, S., Howdle, S., & Illum, L. (2012). PEGylated chitosan derivatives: Synthesis, characterizations and pharmaceutical applications. *Progress in Polymer Science*, *37*, 659-685.

Das, S.N., Madhuprakasha, J., Sarma, P.V.S.R.N., Purushotham, P., Suma, K., Manjeet, K., Rambabu, S., El Gueddari, N.E., Moerschbacher, B.M., & Podile, A.R. (2015). Biotechnological approaches for field applications of chitooligosaccharides (COS) to induce innate immunity in plants. *Critical Reviews in Biotechnologies*, *35*, 29-43.

Dash, M., Chiellini, F., Ottenbrite, R.M., & Chiellini, E. (2011).Chitosan, a versatile semi-synthetic polymer in biomedical applications. *Progress in Polymer Science*, *36*, 981–1014.

Ganji, F., & Abdekhodaie, M.J. (2008). Synthesis and characterization of a new thermosensitive chitosan–PEG diblock copolymer. *Carbohydrate Polymers*, *74*, 435-441.

Guerry, A., Bernard, J., Samain, E., Fleury, E., Cottaz, S., & Halila, S. (2013). Aniline-catalyzed reductive amination as a powerful method for the preparation of reducing end-"clickable" chitooligosaccharides. *Bioconjugate Chemistry*, *24*, 544-549.

Hamed, I., Ozogul, F., & Regenstein, J.M. (2016). Industrial applications of crustacean by-products (chitin, chitosan, and chitooligosaccharides): a review. *Trends in Food Science & Technology, 48*, 40-50.

Huang, H., Jin, Y., Xue, M., Yu, L., Fu, Q., Ke, Y., Chu, C., & Liang, X. (2009). A novel click chitooligosaccharide for hydrophilic interaction liquid chromatography. *Chemical Communications*, 6973-6975.

Hussain, I., Singh, T., & Chittenden, C. (2012). Preparation of chitosan oligomers and characterization: their antifungal activities and decay resistance. *Holzforschung*, *66*, 119–125.

Illy, N., Robitzer, M., Auvergne, R., Caillol, S., David, G., & Boutevin, B. (2014). Synthesis of water-soluble allyl-functionalized oligochitosan and its modification by thiol–ene addition in water. *Journal of Polymer Science, Part A: Polymer Chemistry*, *52*, 39-48.

Kalia, J., & Raines, R. T. (2010). Advances in Bioconjugation. *Current Organic Chemistry*, *14*, 138–147.

Li, K., Xing, R., Liu, S., & Li, P. (2016). Advances in preparation, analysis and biological activities of single chitooligosaccharides. *Carbohydrate Polymers*, *139*, 178-190.

Liu, X.D., Tokura, S., Nishi, N., & Sakairi, N. (2003). A novel method for immobilization of chitosan onto nonporous glass beads through a 1,3-thiazolidine linker. *Polymer*, *44*, 1021-1026.

Liaqata, F., & Eltemb, R. (2018). Chitooligosaccharides and their biological activities: a comprehensive review. *Carbohydrate Polymers*, *184*, 243–259.

Lodhi, G., Kim, Y.S., Hwang, J.W., Kim, S.K., Jeon, Y.J., Je, J.Y., Ahn, C.B., Moon, S.H., Jeon, B.T., & Park, P.J. (2014). Chitooligosaccharide and its derivatives: preparation and biological applications. *BioMed Research International*, Article ID 654913, 13p.

Marzaioli, A.M., Bedini, E., Lanzetta, R., Perino, V., Parrilli, M., & De Castro, C. (2012). Preparation and NMR characterization of glucosamine oligomers bearing an azide function using chitosan. *Carbohydrate Polymers*, *90*, 847- 852.

Mourya, V.K., Inamdar, N.N., & Choudhari, Y.M. (2011). Chitooligosaccharides: synthesis, characterization and applications. *Polymer Science Series A*, *53*, 583-612.

Moussa, A., & Trombotto, S. (2016). Octanoic Hydrazide-Linked Chitooligosaccharides-2,5-anhydro-D-mannofuranose. *Molbank*, M904.

Novoa-Carballal, R., & Müller, A.H.E. (2012). Synthesis of polysaccharide-*b*-PEG block copolymers by oxime click, *Chemical Communications*, *48*, 3781-3783.

Pickenhahn, V.D., Darras, V., Dziopa, F., Biniecki, K., De Crescenzo, G., Lavertu, M., & Buschmann, M.D. (2015). Regioselective thioacetylation of chitosan end groups for nanoparticle gene delivery systems. *Chemical Science*, *6*, 4650-4664.

Pickenhahn, V.D., Grange, M., De Crescenzo, G., Lavertu M., & Buschmann M.D. (2017). Regioselective chitosan end-group activation: the triskelion approach. *RSC Advances*, *7*, 18628-18638.

516 Rhazi, M., Tolaimate, A., Desbrieres, J., Rinaudo, M., Alagui, A., & Vottero, P. (2001).
517 Contribution to the study of the complexation of copper by chitosan and oligomers.
518 *Polymer*, *43*, 1267-1276.

519 Salim, E., Ailincai, D., & Trombotto, S. (2014). Chitooligosaccharide-2,5-anhydro-D-
520 mannonic Acid. *Molbank*, M832.

521 Salim, E., Galais, A., & Trombotto, S. (2014). 4-(Hexyloxy) aniline-linked
522 chitooligosaccharide-2,5–anhydro-D- mannofuranose. *Molbank*, M815.

523 Strand, S.P., Issa, M.M., Christensen, B.E., Vårum, K.M., & Artursson, P. (2008). Tailoring
524 of chitosans for gene delivery: novel self-branched glycosylated chitosan oligomers with
525 improved functional properties. *Biomacromolecules*, 9, 3268-3276.

526 Tømmeraas, K., Vårum, K.M., Christensen, B.M., & Smidsrød, O. (2001). Preparation and
527 characterisation of oligosaccharides produced by nitrous acid depolymerization of
528 chitosans. *Carbohydrate Research*, *333*, 137-144.

529 Tømmeraas, K., Strand, S.P., Christensen, B.E., Smidsrød, O., & Vårum, K.M. (2011).
530 Preparation and characterization of branched chitosans. *Carbohydrate Polymers*, *83*, 1558-
531 1564.

532 Xia, W., Liu, P., Zhang, J., & Chen, J. (2011). Biological activities of chitosan and
533 chitooligosaccharides. *Food Hydrocolloids*, *25*, 170-179.

534 Yang, Y., & Yu, B. (2014). Recent advances in the synthesis of chitooligosaccharides and
535 congeners. *Tetrahedron*, *70*, 1023-1046.

536 Yeul, V.S., & Rayalu, S.S. (2013). Unprecedented chitin and chitosan: a chemical overview.
537 *Journal of Polymers and the Environment, 21*, 606–614.

538 Younes, I., & Rinaudo, M. (2015). Chitin and chitosan preparation from marine sources.
539 Structure, properties and applications. *Marine Drugs*, *13*, 1133-1174.